Available online at www.sciencedirect.com

SCIENCE DIRECT

Biochimica et Biophysica Acta 1665 (2004) 6–19

BIOCHIMICA ET BIOPHYSICA ACTA BBA

http://www.elsevier.com/locate/bba

Simultaneous probing of hydration and polarity of lipid bilayers with 3-hydroxyflavone fluorescent dyes

Andrey S. Klymchenko[a,*], Yves Mély[a], Alexander P. Demchenko[b,c], Guy Duportail[a]

[a] *Laboratoire de Pharmacologie et Physicochimie, UMR 7034 du CNRS, Faculté de Pharmacie, Université Louis Pasteur, BP 60024, 67401 Illkirch, France*

[b] *A.V. Paladin Institute of Biochemistry, 9 Leontovicha str., 01030 Kiev, Ukraine*

[c] *TUBITAK Research Institute for Genetic Engineering and Biotechnology, Gebze-Kocaeli 41470, Turkey*

Received 13 February 2004; received in revised form 15 June 2004; accepted 15 June 2004
Available online 6 July 2004

Abstract

The penetration of water into the hydrophobic interior leads to polarity and hydration profiles across lipid membranes which are fundamental in the maintenance of membrane architecture as well as in transport and insertion processes into the membrane. The present paper is an original attempt to evaluate simultaneously polarity and hydration properties of lipid bilayers by a fluorescence approach. We applied two 3-hydroxyflavone probes anchored in lipid bilayers at a relatively precise depth through their attached ammonium groups. They are present in two forms: either in H-bond-free form displaying a two-band emission due to an excited state intramolecular proton transfer reaction (ESIPT), or in H-bonded form displaying a single-band emission with no ESIPT. The individual emission profiles of these forms were obtained by deconvolution of the probes' fluorescence spectra. The polarity of the probe surrounding the bilayer was estimated from the two-band spectra of the H-bond-free form, while the local hydration was estimated from the relative contribution of the two forms. Our results confirm that by increasing the lipid order (phase transition from fluid to gel phase, addition of cholesterol or decrease in the lipid unsaturation), the polarity and to a lesser extent, the hydration of the bilayers decrease simultaneously. In contrast, when fluidity (i.e. lipid order) is kept invariant, increase of temperature and of bilayer curvature leads to a higher bilayer hydration with no effect on the polarity. Furthermore, no correlation was found between dipole potential and the hydration of the bilayers.

Keywords: Fluorescent membrane probe; 3-Hydroxyflavone; Membrane polarity and hydration

1. Introduction

Polarity and hydration are two fundamental physicochemical characteristics of the lipid bilayer. According to the classical model of lipid bilayers, these two parameters exhibit a strong gradient across the bilayer, so that polarity and hydration are extremely low at the bilayer center, due to hydrophobic interactions of the fatty acid chains, and very high at the bilayer interface, due to interactions of water with the lipid head groups [1]. The polarity and hydration gradients are responsible for the formation of specific gradients of electric field across the membrane, such as surface and dipole potentials [2–4]. Polarity, hydration and electric potential gradients control many processes like membrane transport, ion conductance and insertion of proteins and other molecules into membranes and their translocation across the membrane [5,6]. Therefore, the study of these properties at precise bilayer depths is of peculiar importance for understanding the mechanisms of biomembrane functions.

A number of experimental methods have been applied to study hydration and polarity in the bilayer, such as EPR [7,8], NMR [9,10], IR [11,12] and fluorescence spectroscopies. Among them, the most popular is fluorescence spectroscopy with the use of polarity-sensitive (solvatochromic) fluorescent probes [13]. The most commonly applied probes of this type are Prodan [14,15], Laurdan [16,17], NBD [18,19], dansyl [20,21] and anthroyloxy [22,23] derivatives. Thus, Prodan and Laurdan can be used to follow changes in bilayer polarity and hydration on phase transition, phase fluctuation, formation of lipid domains and addition of cholesterol [14–17]. NBD and dansyl fluoro-

* Corresponding author. Tel.: +33-390-24-41-15; fax: +33-390-24-43-12.
E-mail address: aklymchenko@aspirine.u-strasbg.fr (A.S. Klymchenko).

0005-2736/$ - see front matter © 2004 Elsevier B.V. All rights reserved.
doi:10.1016/j.bbamem.2004.06.004

phores attached to lipid head groups are also frequently used to study the polarity and hydration of the bilayer [18,19,21]. However, the latter dyes are significantly less solvatochromic and their high polarity makes them applicable mainly to study membrane interfaces [21,22]. The anthroyloxy fluorophore is significantly less polar and thus its conjugates with fatty acids allow following polarity at different depths in lipid bilayers [23,24].

Despite the popularity of these probes in a number of applications, none of them allow discrimination between polarity and hydration effects. Polarity as it is recorded by the fluorescent probes is an integrated function, which describes the ability of the surrounding molecules to dielectrically stabilize the ground and excited state dipoles of the probes [25–27]. Hydration water can also contribute to this stabilization, since water molecules could form a highly dielectric environment. In addition, they can provide specific H-bonding interactions with fluorescent probes resulting in changes of intensity and shifts of emission bands, i.e. of the same parameters that are used for evaluation of polarity changes. For instance, H-bonds between Prodan and protic solvent molecules induce a red shift of almost 50 nm, which corresponds to about half of the total solvatochromic response of this probe [28–30]. Therefore, the apparent ''polarity'' obtained by using these probes serves as an integrated function of both the classical polarity (approximated by the Onsager function of dielectric constant [25,26]) and the H-bonding effects. For most solvatochromic probes, the H-bonding effects are mainly determined by the H-bond donor ability of the surroundings [27–29,31,32], since these dyes are generally H-bond acceptors in their ground and excited states. Inside the lipid bilayer, the H-bonding effects are mainly determined by the concentration of embedded water molecules since most of the lipids do not contain H-bond donor groups located deeper than the charged lipid heads. Meantime, the polarity at a particular depth of the bilayer depends on the presence of polar groups or molecules and by their relative mobility [7,16,17,33]. These considerations emphasize the importance of separately determining polarity and hydration.

The separate determination of polarity and hydration in the bilayers requires fluorescent dyes with a sufficient number of appropriate spectroscopic parameters. In this respect, the most prospective dyes are 3-hydroxyflavone derivatives. These dyes display an excited state intramolecular proton transfer reaction (ESIPT) (Scheme 1), which results in dual fluorescence with two highly resolved emission bands [34]. The short-wavelength band corresponds to emission of the normal (N*) excited state, while the long-wavelength band originates from the tautomer (T*, ESIPT product) state (Scheme 1). The position of these bands as well as their relative intensities are highly sensitive to polarity and H-bonding effects, thus allowing the development of algorithms that discriminate between these two effects [35,36]. Thus an increase in polarity results in an increase of the relative intensity of the N* band accompanied by its strong red shift. Furthermore, the formation of intermolecular H-bonds with protic solvent (water or alcohols) results in a nearly complete switch of the ESIPT and therefore induces a strong increase of the relative intensity of the N* emission [35,38]. 3-Hydroxyflavones have already been applied for biophysical studies

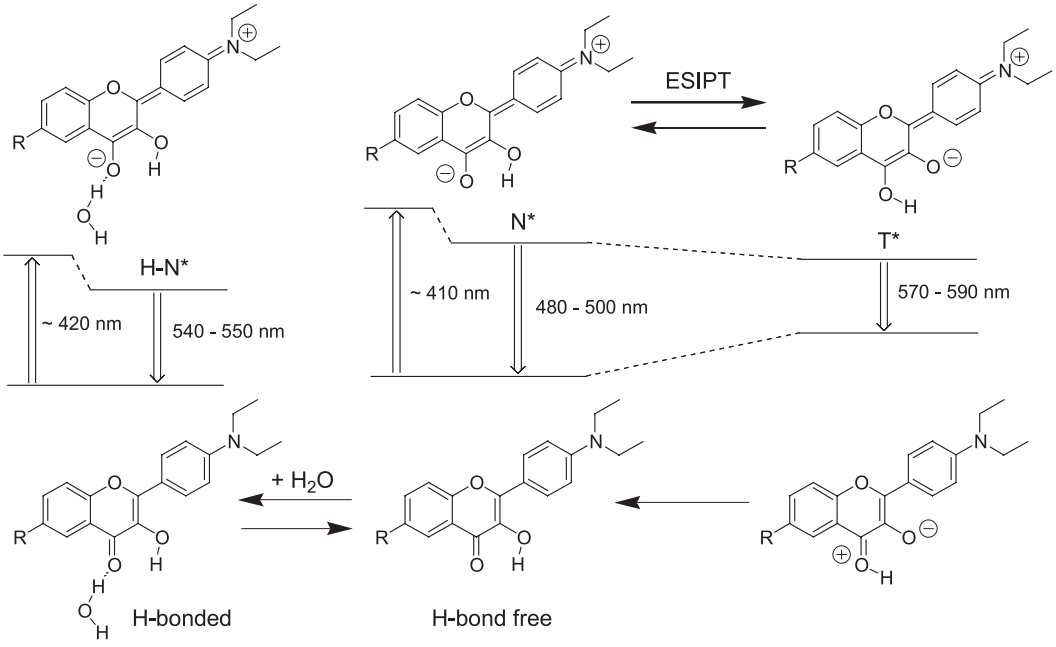

Scheme 1. Ground (below) and excited (above) states of 4′-diethylamino-3-hydroxyflavone dye as well as schematic presentation of its energy levels. Upward arrows represent excitation process to the Frank–Condon excited state, while downward arrows represent emission process. The correspondent band maxima (in nanometers) are indicated.

of lipid bilayers. For instance, the simple neutral probe 4′-dimethylamino-3-hydroxyflavone (F) (Fig. 1) was used to follow the interdigitation process in the bilayer [37] and the effects of cholesterol [37], lipid composition and surface charge [38]. Recently, by using this probe, we made a first attempt to analyze simultaneously the polarity and hydration in the lipid bilayer [39]. We found that the probe hydration is connected with the heterogeneity of probe location, since the hydrated form of the probe is located at the polar membrane interface, while the non-hydrated (H-bond-free) form is more deeply embedded into the bilayer. Furthermore, the analysis of the literature allowed us to conclude that such a bimodal distribution in the bilayer is probably a general feature of neutral solvatochromic probes containing H-bond acceptor groups, including Prodan, Laurdan, Nile Red, etc. These molecules are distributed in the bilayer along the polarity and hydration gradients [39], a feature which may lead to artifacts in the estimation of the latter parameters. In order to provide a precise location to the fluorophore at a particular depth, the probe should be anchored with a charged group. This idea has already been applied to the Prodan derivative, Patman, with the introduction of a positively charged ammonium group that can interact with the phosphate groups of lipids [40]. Charged groups were also used to locate the anthroyloxy fluorophore at different bilayer depths [23,24] and the coumarin fluorophore at a particular distance from the bilayer interface [41], as well as to provide a vertical orientation to styrylpyridinium dyes [42]. In this context, we recently developed two 3-hydroxyflavone derivatives containing cationic ammonium groups, F2N8 and F4N1 [43]. These two probes (Fig. 1) present a much more precise location and orientation in the lipid bilayer as compared to the neutral analog F [43]. Especially, the vertical orientation achieved with F4N1 allowed us to apply this probe as a highly sensitive tool for measuring the membrane dipole potential [44].

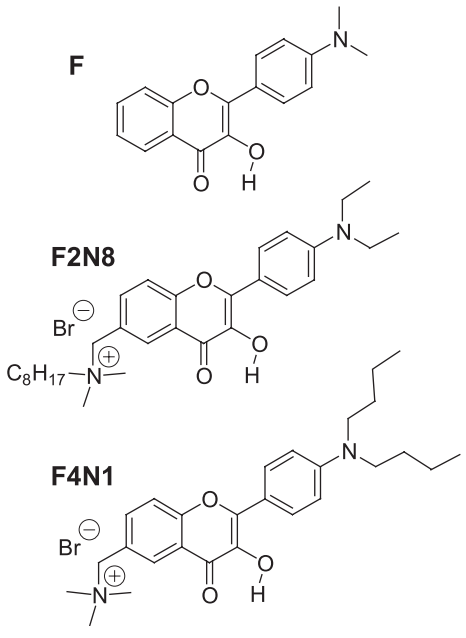

Fig. 1. Chemical structure of studied probes.

In the present work, we attempt to study with probes F2N8 and F4N1 both the polarity and the hydration of phospholipid bilayers. We show that these two parameters can be studied simultaneously with a single probe. Their separate characterization provides new insights in understanding the structure and functions of lipid bilayers and biomembranes.

2. Materials and methods

Dilauroyl-, dimyristoyl-, dipalmitoyl-, and dioleoyl phosphatidylcholine (DLPC, DMPC, DPPC and DOPC, respectively), egg yolk phosphatidylcholine (EYPC), and cholesterol were purchased from Sigma-Aldrich Co. (Lyon, France). 1-Palmitoyl-2-oleoyl-*sn*-glycero-3-phosphotempocholine (TempoPC), 1-palmitoyl-2-(5- and 12-doxyl)-stearoyl-*sn*-glycero-3-phosphocholine (5- and 12-SLPC) and 1,2-Di-*o*-tetradecyl-*sn*-glycero-3-phosphocholine (DTPC) were purchased from Avanti Polar Lipids (Alabaster, AL, USA). Probes F2N8 and F4N1 were synthesized and purified as previously described [43]. The probe samples were pure according to thin-layer chromatography (TLC), ^{1}H-NMR, absorption and fluorescence spectra in organic solvents.

Large unilamellar vesicles (LUV) were obtained by the extrusion method as previously described [45]. Briefly, a suspension of multilamellar vesicles was extruded by using a Lipex Biomembrane extruder. The size of the filters was first 0.2 μm (7 passages) and thereafter 0.1 μm (10 passages). Typically, this procedure generates monodisperse unilamellar vesicles with a mean diameter of 0.11 μm, as measured with a Zetamaster 300 (Malvern Instruments).

LUVs were labeled by adding an aliquot (generally 2 μl) of probe stock solution (2 mM) in dimethyl sulfoxide to 2 ml vesicle suspensions. Since the binding kinetics was very rapid, the fluorescence spectra were recorded a few minutes after addition of the probe. The depths of the probe molecules in the bilayer were measured by the parallax quenching method [46] by using TempoPC, 5- and 12-SLPC as quenchers at a molar ratio of 15%, as previously described [43,47]. A 15 mM HEPES, pH 7.4 buffer was used in all the experiments. Concentrations of the probes and lipids were 2 and 200 μM, respectively.

Fluorescence spectra were recorded on an SLM-Aminco 48 000 (Urbana-Champaign, IL, USA) spectrofluorometer and corrected by subtracting the spectra of the corresponding blank vesicles. The fluorescence anisotropy spectra were determined on an SLM-Aminco 8000 spectrofluorometer in its L-configuration, the excitation polarizer being vertically oriented, by recording the emission fluorescence spectra with the emission polarizer oriented

first vertically, then horizontally. The combination of these two emission spectra, after taking into account the correction factor obtained by orienting the excitation polarizer horizontally, leads to the anisotropy spectra. The excitation wavelength was 400 nm unless otherwise indicated.

Deconvolution of the probes fluorescence spectra into three bands, corresponding to normal (N*), normal H-bonded (H-N*) and tautomer (T*) forms, was performed by using the "Siano" software kindly provided by its author (Dr. A.O. Doroshenko, Kharkov, Ukraine) [48]. The program is based on an iterative non-linear least-squares method based on the Fletcher–Powell algorithm. The individual emission bands were approximated by a log-normal function [49]. The quadriparametric (maximal amplitude, I_{max}, spectral maximum position, ν_{max}, and positions of half-maximal amplitudes, ν_1 and ν_2, for the blue and red parts of the band, respectively) log-normal function has been proposed by Siano and Metzler [49] for describing the absorption spectra of complex molecules and was later successfully used to resolve multicomponent absorption and fluorescence spectra in biological systems [48–52]. Unlike commonly used Gaussian functions, log-normal functions allow accounting for the band asymmetry. The program "Siano" operates with the shape parameters of the log-normal function that are directly connected with the abovementioned parameters: full width at half maximum, $FWHM = \nu_1 - \nu_2$, and band asymmetry, $P = (\nu_1 - \nu_{max})/(\nu_{max} - \nu_2)$, and allows approximating the asymmetric bands in absorption and fluorescence spectra [48]. This program also allows keeping one fixed or several spectroscopic parameters in order to obtain more stable results of deconvolution, insofar as these fixed values are justified by comparative analysis and physical modeling. In our case, the adopted fixed values are physically justified based on previously obtained data in organic solvents and LUVs [35,39]. Thus, for the iteration process, the FWHM of the two short-wavelength bands (N* and H-N*) were fixed at 3000 cm^{-1}. For the H-N* band, the asymmetry and the band position were fixed at 0.9 and 18 400 cm^{-1}, respectively. The other parameters, i.e. asymmetry of N* and T* bands, band width of the T* band and relative intensities of the bands, were allowed to vary in the iteration process. The same deconvolution procedure was applied to the spectra obtained during parallax quenching experiments. The quenching efficiencies of the individual forms of the probes were estimated from the changes in the integral intensities of the deconvoluted bands.

3. Results

3.1. Hydrated and non-hydrated forms of the probes

The probe F2N8 in EYPC vesicles shows a strong dependence of the emission spectrum on the excitation wavelength (Fig. 2). Indeed, shifting the excitation wavelength from 400 nm (short-wavelength edge) to 440 nm (long-wavelength edge) results in a dramatic decrease of the T* emission accompanied by a red shift of the short-wavelength band and the disappearance of its short-wavelength shoulder (Fig. 2). This result cannot be explained by the classical red-edge effect in rigid media [53] and suggests the presence of several ground state forms differing by the position of their absorption maximum. In line with our previous studies with dye F in lipid vesicles [39], this ground state heterogeneity may be connected with the presence of H-bonded and H-bond-free forms of the probe in the bilayer. Absorption maximum of the former is shifted to the red (ca. 10 nm) with respect to the H-bond-free form [35,36], and therefore the excitation at the red edge of the spectrum photo-selects the H-bonded form, which does not readily undergo ESIPT reaction and thus exhibits a single emission band (H-N*) [35]. According to the data obtained with F2N8 in a protic solvent ethanol (emission maximum = 543 nm), the H-N* band should locate around 540–550 nm. Interestingly, the fluorescence spectrum of F4N1 in EYPC vesicles presents much less pronounced excitation wavelength dependence (Fig. 2B). This may be explained by the deeper location of the probe in the bilayer [43], so that the H-bond-free form of the probe dominates in the emission spectra.

To confirm the existence of different emissive forms, we recorded the fluorescence anisotropy spectrum for both probes. For flavone dyes in a restricted medium, with only the presence of the N* and T* emission bands, one should

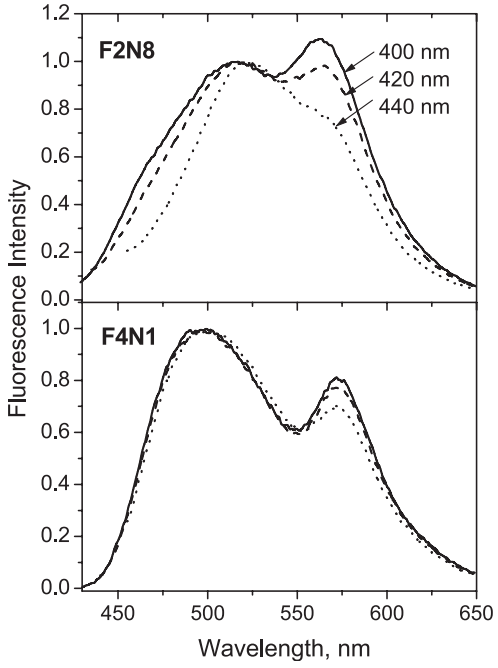

Fig. 2. Fluorescence spectra of probes F2N8 and F4N1 in EYPC vesicles as a function of the excitation wavelength.

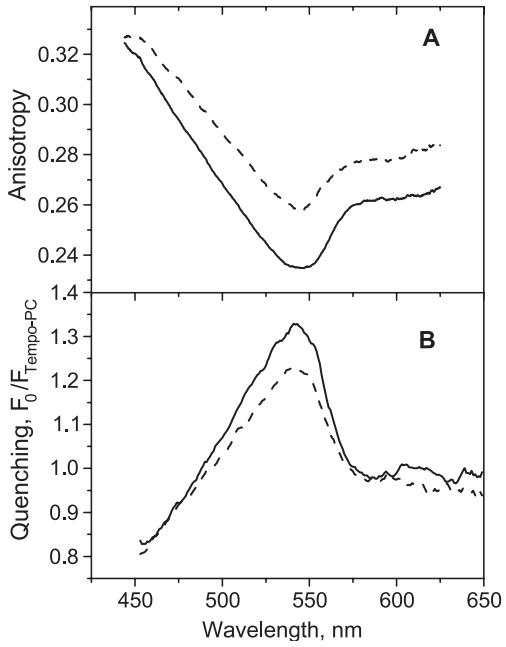

Fig. 3. Evidence of the heterogeneity in emission spectra of probes F2N8 (solid line) and F4N1 (dashed line) in LUV. (A) Fluorescence anisotropy emission spectra in EYPC vesicles; (B) fluorescence quenching as function of wavelength in DOPC vesicles with 15% Tempo-PC as surface quencher.

expect a rather high emission anisotropy for the N* band and a much lower one for the T* band [39]. Furthermore, fluorescence anisotropy should be constant over the emission band corresponding to a single electronic transition, and anisotropy changes should be observed only for the overlapping wavelengths of N* and T* bands. Our results (Fig. 3) show that for both F2N8 and F4N1 probes, the emission anisotropy decreases strongly across the short-wavelength emission band and reaches a minimal value at around 543 nm. This constitutes a direct evidence for the contribution to the fluorescence spectra of both probes of a species with low emission anisotropy, for which the maximum of emission should be at about 543 nm. Remarkably, the maximum of this additional band is exactly the same as that of the H-bonded species of the studied probes in ethanol.

With the neutral probe F, we have previously shown that the H-bonded form locates at the polar membrane interface, while the H-bond-free form is deeply embedded in the hydrophobic region of the bilayer [39]. Some heterogeneity of locations may also occur for the two present probes, in spite of their anchoring to the bilayer interface. To test this hypothesis, we first performed a fluorescence quenching experiment by using TempoPC containing the nitroxide quencher group located at the bilayer interface. The results show that the quenching depends strongly on the emission wavelength (Fig. 3B), with the highest efficiency at about 543 nm. Thus, the profile of quenching efficiency is very similar to that of emission anisotropy, demonstrating that the H-bonded forms of both probes (emitting around 543 nm) may present shallower locations than the corresponding H-bond-free forms.

Thus, in order to describe the complex emission spectra of the 3-hydroxyflavone probes F2N8 and F4N1 in lipid bilayers, three emission bands must be considered. The two bands at 480–500 and 570–580 nm correspond to emission of the classical normal (N*) and tautomer (T*) excited state forms that do not possess intermolecular H-bonds. These two forms are coupled by ESIPT (Scheme 1) and their relative intensities should correlate strongly with surrounding polarity. The third band with the maximum at ca. 543 nm corresponds to the normal H-bonded species (H-N*) of the dyes. With respect to the N* state, the H-N* state is energetically stabilized by the intermolecular H-bonding with a water molecule (Scheme 1) and therefore its ESIPT is probably not favored [35]. We do not consider other H-bonded forms to contribute to the observed emission spectrum because according to our recent studies of 3-hydroxyflavone derivatives in organic solvents, only the H-bonded species that is presented in Scheme 1 are actually observed in emission [36]. Furthermore, we do not consider protonated or deprotonated forms to contribute to the emission spectra since they are not detectable in the excitation spectra in the pH range of this study.

In order to further characterize the emissive species of the probes, we deconvoluted the emission spectra into three bands using log-normal functions [49]. To provide the most accurate and physically justified deconvolution, we have to select optimal parameters (band maximum, FWHM and asymmetry) for each of the log-normal components. According to our data in neat solvents and lipid bilayers [35,39], the shape of the N* band in lipid vesicles does not differ significantly from that observed in protic solvents, so that their asymmetry and FWHM are approximately the

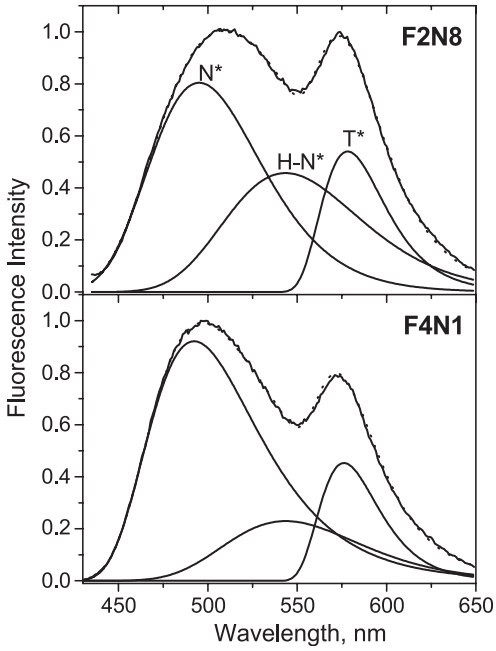

Fig. 4. Fluorescence spectra of probes F2N8 and F4N1 in EYPC vesicles and their deconvolution into the N*, H-N* and T* bands.

same, ca. 0.8–0.9 and 2500–3000 cm^{-1}. In contrast, the T* band exhibits a much higher asymmetry, ca. 0.70, and around 2.5 times smaller FWHM, ca. 1400 cm^{-1} (the corresponding values in ethyl acetate are 0.70 and 1380 cm^{-1}). In this respect, to deconvolute the fluorescence spectra of the probes in lipid vesicles, we fixed the FWHM of the N* band at 3000 cm^{-1}. For the H-N* bands, we fixed the FWHM, asymmetry and position at 3000 cm^{-1}, 0.9 and 18400 cm^{-1}, respectively. The latter value, corresponding to 543 nm, was chosen according to the anisotropy and quenching data. The other parameters (i.e. asymmetry of the N* and T* bands, band width of the T* band and relative intensities of the bands) were allowed to vary during the iteration process. For all the studied lipid vesicles, the deconvolution of the fluorescence spectra into three bands yielded an excellent correlation parameter ($r^2 \geq 0.999$). As an example, the deconvoluted bands for EYPC vesicles are presented in Fig. 4. We analyzed the fluorescence spectra of probes F2N8 and F4N1 in lipid vesicles differing in phase state, fatty acids composition and the presence of cholesterol. Some of the spectroscopic data were obtained in our previous studies [43,44]. The results are presented in Table 1. We observe that the position and shape of the bands are similar in different lipid vesicles, and that the differences in the shape of emission spectra result from differences in the relative intensities of the three emission bands (Tables 1 and 2).

3.2. Polarity and hydration of the bilayer and location of the probes

According to the above fluorescence quenching data, the H-bonded form of the probes seems to be located shallower than their corresponding H-bond-free form. Then the question arises why probes carrying charged anchoring groups exhibit such heterogeneity in their location. Based on the distribution of polar and apolar groups in the probes structure, one can expect that the fluorophore moiety may orient more or less vertically with respect to the bilayer surface (Fig. 5). The more vertical orientation with a deeper embedding may correspond to the H-bond-free form, while the H-bonded form may orient in a more tilted way, closer to the polar interface (Fig. 5). With the purpose to determine the depths of H-bonded and H-bond-free forms in the lipid bilayer, we reanalyzed a set of previous quenching data obtained for probes F2N8 and F4N1 in DOPC bilayers, by using as nitroxide quenchers not only TempoPC, but also 5-SLPC and 12-SLPC [43]. For this purpose, we considered separately the quenching efficiencies of the deconvoluted bands of the H-bond-free

Table 2
Polarity and hydration parameters, I_{N*}/I_{T*} and F_B/F_F, obtained with probes F2N8 and F4N1 in lipid vesicles

Sample[a]	F2N8		F4N1	
	I_{N*}/I_{T*} Polarity	F_B/F_F Hydration	I_{N*}/I_{T*} Polarity	F_B/F_F Hydration
EYPC, SUV	1.60	1.270	2.44	0.604
EYPC (20 °)	1.50	0.452	2.03	0.208
EYPC (50 °)	1.53	0.793	2.36	0.384
EYPC-Chol	1.03	0.414	1.37	0.139
EYPC-6KC	0.80	0.382	0.75	0.146
DOPC (20 °)	1.78	0.625	2.67	0.182
DLPC (25 °)	1.00	0.484	1.44	0.196
DMPC (15 °)	0.91	0.594	1.12	0.314
DMPC (38 °)	1.07	0.661	1.61	0.345
DPPC (48 °)	1.11	0.911	1.50	0.493
DTPC (15 °)	1.82	0.360	2.84	0.109
DTPC (38 °)	1.95	0.464	3.15	0.138

[a] The samples are the same as in Table 1.

Table 1
Spectroscopic characteristics of probes F2N8 and F4N1 in lipid vesicles[a]

Sample[b]	F2N8						F4N1					
	λ_{ex} (nm)	λ_{N*} (nm)	λ_{T*} (nm)	P_{N*}	P_{T*}	W_{T*} (cm^{-1})	λ_{ex} (nm)	λ_{N*} (nm)	λ_{T*} (nm)	P_{N*}	P_{T*}	W_{T*} (cm^{-1})
EYPC, SUV	–	496	580	0.89	0.76	1260	–	493	576	0.84	0.67	1200
EYPC[c]	419	495	579	0.89	0.70	1260	420	493	576	0.80	0.70	1210
EYPC (50 °C)	418	496	580	0.97	0.75	1310	420	493	578	0.86	0.79	1310
EYPC-Chol	419	492	579	0.80	0.72	1250	420	490	576	0.72	0.70	1230
EYPC-6KC[d]	415	493	578	0.93	0.70	1350	412	486	574	0.81	0.69	1340
DOPC[c]	419	494	580	0.84	0.75	1220	420	492	577	0.80	0.69	1270
DLPC (25 °C)	415	493	577	0.91	0.70	1310	416	489	575	0.78	0.68	1290
DMPC (15 °C)	417	497	578	0.90	0.74	1270	417	489	575	0.83	0.70	1270
DMPC (38 °C)	415	493	578	0.87	0.75	1300	416	489	575	0.81	0.70	1240
DPPC (48 °C)	415	496	578	0.91	0.74	1280	416	493	576	0.87	0.73	1280
DTPC (15 °C)	–	496	578	0.90	0.68	1270	–	494	578	0.81	0.70	1230
DTPC (38 °C)	422	492	580	0.89	0.72	1300	426	492	579	0.79	0.72	1260

[a] λ_{ex}—position of the maximum of the excitation spectrum recorded at the T* band maximum; λ_{N*}, and λ_{T*}—positions of the maximum of the N* and T* emission bands, respectively; P_{N*} and P_{T*}—asymmetry of the N* and T* bands, respectively; W_{T*}—FWHM of the T* band. All the values except λ_{ex} are obtained from the deconvoluted spectra.

[b] SUV and LUVs were studied at room temperature (20 °C) unless indicated; cholesterol and 6-KC are present at 30% molar ratio.

[c] Original spectroscopic data were previously reported in Ref. [43].

[d] Spectroscopic data from Ref. [44].

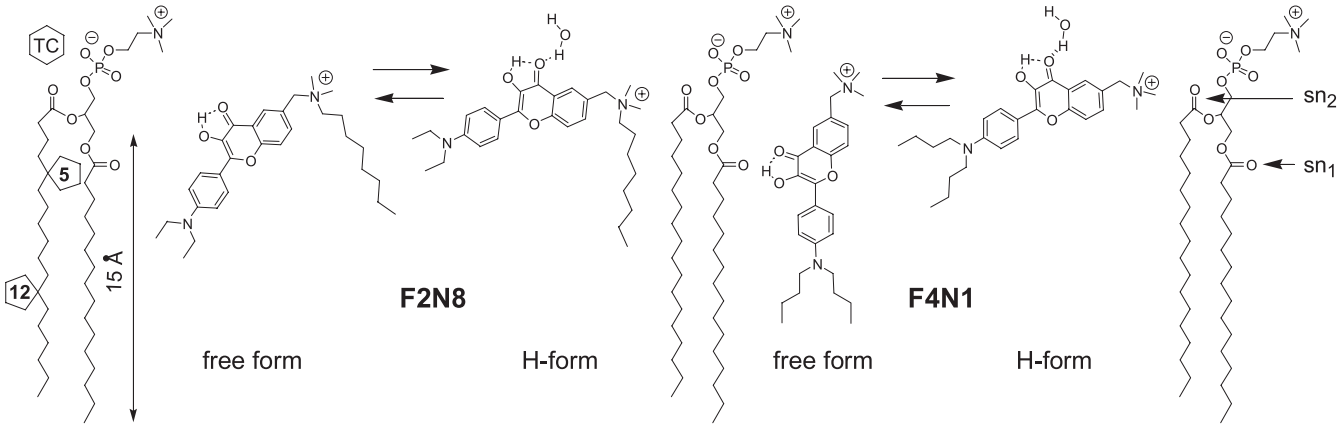

Fig. 5. Estimated location of H-bonded and H-bond-free forms of probes F2N8 and F4N1 in a PC lipid bilayer. The location of phospholipid functional groups is based on the study of Wiener and White [54]. The location of nitroxide paramagnetic quenchers is shown as five- or six-membered rings on the left side.

form (N* + T*) and the H-bonded form (Table 3). This analysis shows that the H-bond-free form of F4N1 is located deeper in the bilayer (9.5 Å from the center of the bilayer) than the H-bond-free form of F2N8 (13 Å). These data suggest that the H-bond-free form of probe F4N1 may be vertically oriented in the bilayer, while that of F2N8 may present a tilted orientation (Fig. 5), in line with our previous conclusions [43]. In contrast, the H-bonded forms of both dyes show similar locations in the region close to phospholipid ester groups of the bilayer. The shallow location of the hydrophobic probe F4N1 is probably energetically unfavorable, explaining the low fraction of H-bonded form with this dye. Meantime, chemical structure of probe F2N8 does not support its vertical orientation in the bilayer (Fig. 5) [43], and, as a result, both H-bonded and H-bond-free forms are rather shallow located, with only 3 Å depth difference. The relative concentration of the two forms, [H-bonded probe]/[H-bond-free probe], is determined mainly, if not only, by the hydration level of the probe environment. Because F2N8 presents nearly the same location for both H-bonded and H-bond-free forms, it is more advantageous for probing hydration at a particular depth, in comparison with probe F4N1 and neutral probe F [39].

Table 3
Fluorescence quenching parallax data on probes F2N8 and F4N1[a]

Dye form	F_{TC}/F_0	F_5/F_0	F_{12}/F_0	Z_{cf} (Å)
F2N8[b]	0.53	0.49	0.59	15
H-bonded F2N8	0.34	0.31	0.43	16
H-bond free F2N8	0.676	0.41	0.58	13
F4N1[b]	0.53	0.43	0.47	10
H-bonded F4N1	0.25	0.33	0.42	17
H-bond free F4N1	0.58	0.45	0.46	9.5

[a] F_{TC}/F_0, F_5/F_0, and F_{12}/F_0 are the values of fluorescence quenching ratios in vesicles containing 15 mol% TempoPC, 5-SLPC and 12-SLPC, respectively, to DOPC vesicles lacking nitroxide-labeled lipid. The values were obtained by deconvolution of the fluorescence quenching data obtained previously [43]. The integral intensities of the H-N* band and the sum of the integral intensities of N* and T* bands were used to calculate the quenching for the H-bonded and H-bond free forms, respectively, of both probes. Z_{cf} is the distance between the middle of the bilayer and the chromophore center calculated from the parallax equation [47].

[b] Data from Ref. [43].

The distribution between the hydrated and non-hydrated forms of the probes in the lipid bilayer can be further analyzed by calculating the relative integral intensities of H-N*, N* and T* bands obtained by deconvolution of the experimental spectra. Since the FWHMs of the N* and H-N* bands are close to each other and are 2.5 times as wide as that of the T* band (not shown), it is then possible to calculate the approximate partition of probes F2N8 and F4N1 between hydrated and non-hydrated forms from the following equation:

$$\frac{[B]}{[F]} = C\frac{Q(F)}{Q(B)}\frac{\int I_{HN^*}d\lambda}{\int I_{N^*}d\lambda + \int I_{T^*}d\lambda} \cong C\frac{Q(F)}{Q(B)}\frac{I_{HN^*}}{I_{N^*} + 0.4I_{T^*}}, \quad (1)$$

where [B] and [F] are the concentrations of the probe in H-bonded and H-bond-free forms, respectively, C is a constant corresponding to the ratio of molar absorptivities of the H-bonded and H-bond-free forms of the probe at the excitation wavelength, and Q(F) and Q(B) are their respective fluorescence quantum yields. However, the absolute value of the [B]/[F] ratio could not be calculated since the ratio of quantum yields, $Q(F)/Q(B)$, is not known and cannot be easily determined. Nevertheless, if we assume that the ratio of quantum yields does not change substantially from one type of lipid vesicles to another (unless specific quenching effects are involved), the intensity ratio $F_B/F_F = I_{H\text{-}N^*}/(I_{N^*} + 0.4I_{T^*})$ could serve as a relative parameter for the probe (and accordingly the bilayer) hydration.

The other important spectroscopic parameter is the intensity ratio of the N* and T* emission bands of the H-bond-free form of the probes, I_{N^*}/I_{T^*}. According to our previous studies, this parameter is a sensitive indicator of the environment polarity [35]. Both the I_{N^*}/I_{T^*} and F_B/F_F

ratios can be obtained directly from the fluorescence spectrum by the deconvolution analysis. Thus, this approach allows us to study simultaneously polarity and hydration at the bilayer depths corresponding to the fluorophore location. In the case of F2N8 and F4N1, polarity is estimated at the depths of the H-bond-free forms at 13 and 9.5 Å, respectively. Similarly, hydration can be estimated only for the particular range of the bilayer depths which is determined by the location of H-bonded and H-bond-free forms. For F2N8 and F4N1, this range is about 13–16 and 9.5–17 Å, respectively.

The unique feature of our approach is that the I_{N*}/I_{T*} ratio describes only non-specific dipole–dipole interactions of the probe with its environment, while the specific interaction (H-bonding) of the probe with water is estimated with the F_B/F_F ratio. It is also important to note that, especially for the probe F4N1 presenting a vertical orientation of the fluorophore moiety in the bilayer, the bilayer dipole potential may contribute to the polarity parameter, I_{N*}/I_{T*}. It is well known that at the depth of F4N1 location, the environment is highly anisotropic, so that the electric field vector inducing the dipole potential is inversely oriented to the probe excited state dipole. As a consequence, an increase in the dipole potential should result in the decrease of the I_{N*}/I_{T*} ratio [44], which is apparently opposite to the polarity effect. As it will be shown below, the polarity and dipole potential effects can be easily distinguished based on analysis of the excitation spectra.

We applied this new probing methodology to analyze simultaneously the polarity and hydration in a variety of lipid bilayers. The calculated values of polarity (expressed as I_{N*}/I_{T*}) and hydration (expressed as F_B/F_F) of different lipid bilayers are presented in Table 2. As a general trend, it can be seen that the hydration measured by probe F4N1 is much lower than the one measured by probe F2N8 for all the studied vesicles, in excellent agreement with the deeper average location of the former probe (Table 3). However, the absolute values of the I_{N*}/I_{T*} ratio cannot be compared for these two probes because, as the probe F4N1 is located in a more hydrophobic environment, the internal Stark effect of the positively charged group [55] should be more pronounced for this probe than for F2N8, and thus could explain the abnormally high values of the I_{N*}/I_{T*} ratio for the former (Table 2). Indeed, the considerably larger values of the I_{N*}/I_{T*} ratio observed for F4N1 as compared to F2N8 may be the result of inhibition of the ESIPT reaction due to the proximity of 3-OH group of the flavone moiety to the sn_1-carbonyl groups in the bilayer [43]. Thus, it is useful to compare not the absolute values of the corresponding ratios for these two probes, but their relative changes.

3.3. Probing structural modifications in the bilayer

3.3.1. Surface curvature: comparison of SUV and LUV

Fluorescence spectra of probes F2N8 and F4N1 in SUV and LUV are presented in Fig 6A and D. For both probes, it can be noticed that the two emission bands are better resolved in LUV than in SUV. The deconvolution data clearly show that SUV as compared to LUV are characterized by much larger values of the hydration parameter F_B/F_F for both probes, while the polarity parameter I_{N*}/I_{T*} is not significantly different (Table 2). This is in line with the high curvature of the SUV bilayer, which renders the interfacial region of the bilayer more accessible to water molecules, without affecting the dielectric properties and mobility of the inner regions.

3.3.2. Phase transition and temperature effects

As for the increase in the bilayer curvature, the phase transition of lipid bilayers from gel to liquid crystalline phase results in an apparent decrease of the resolution of the two bands in the emission spectra of both F2N8 and F4N1 (Fig. 6B,E). The deconvolution data show an increase of both F_B/F_F and I_{N*}/I_{T*} ratios upon the transition (Table 2). These data demonstrate that the region at 9–16 Å from the bilayer center is characterized by a higher polarity and hydration in the liquid crystalline phase than in the gel phase. It should be noted that the increase of the polarity parameter I_{N*}/I_{T*} on the phase transition is considerably higher with probe F4N1 (Table 2), indicating that the polarity increase is more pronounced at the deeper region of the bilayer.

An interesting observation can be made by comparing LUVs made from several saturated phosphatidylcholines differing in their fatty acid chain lengths, namely DLPC, DMPC and DPPC. These LUVs were studied in their liquid crystalline phase, at "equivalent" temperatures (25, 38 and 48 °C, respectively). At these temperatures, the different LUVs exhibit the same bilayer fluidity as measured by 1,6-diphenyl-1,3,5-hexatriene (DPH) fluorescence anisotropy ($r_{DPH} = 0.10$). In these conditions, we observe for the three types of vesicles similar values of bilayer polarity as assessed from the I_{N*}/I_{T*} ratios of both probes (Table 2). In contrast, the strong F_B/F_F increase from DLPC to DPPC demonstrates an increase in the hydration of the bilayer ester region with temperature (Table 2).

This interesting difference in the profiles of hydration and polarity prompted us to study the temperature effects on vesicles made from unsaturated lipids. In EYPC vesicles, the increase in temperature also induces a strong decrease of the resolution between the two emission bands for both probes (Fig. 6C,F). The deconvolution data further show that the temperature increase provides only a minor increase in the polarity parameter I_{N*}/I_{T*}, while the hydration parameter F_B/F_F increases dramatically (Table 2). Thus, independently of the nature (saturated or unsaturated) of the lipids, we observe that in the ester region of the lipid bilayer (9–16 Å from the bilayer center) the temperature induces a strong increase in hydration with only a minor effect on the polarity.

3.3.3. Influence of lipid unsaturation degree

According to our previous data, the deeply located form of neutral probe F shows a significant polarity

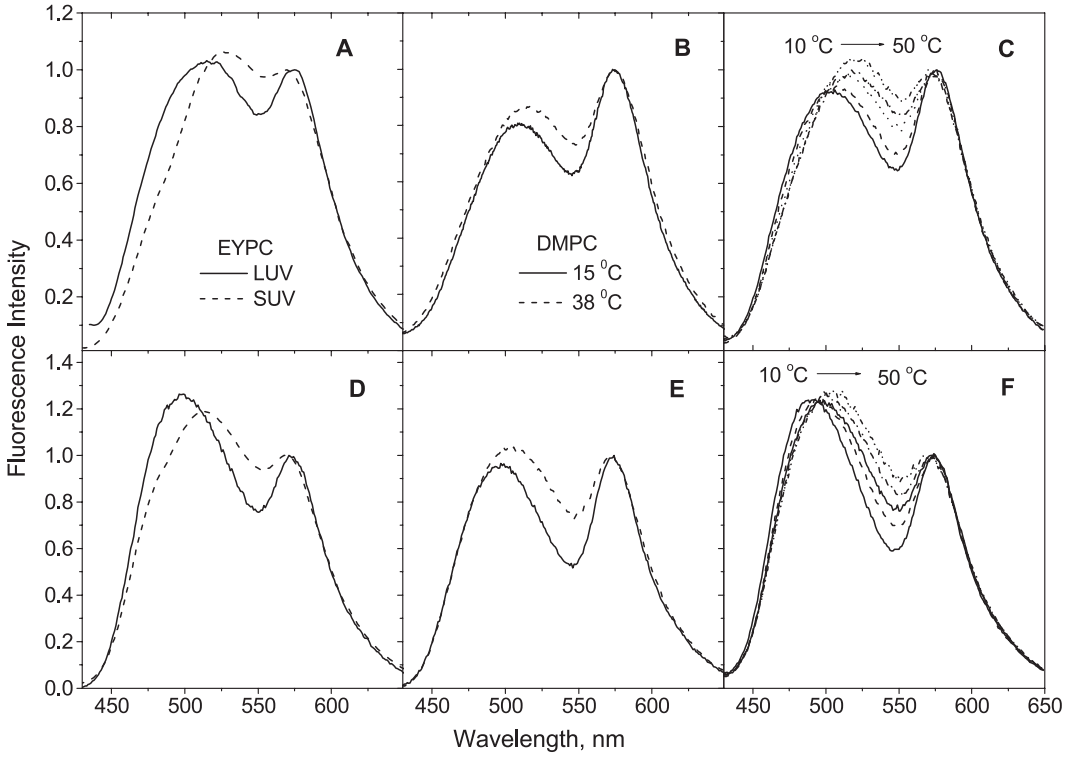

Fig. 6. Fluorescence spectra of probes F2N8 (A–C) and F4N1 (D–F) in lipid vesicles. (A and D) EYPC LUV (solid) and SUV (dash); (B and E) DMPC vesicles at 15 °C (solid) and 38 °C (dash); (C and F) EYPC vesicles at different temperatures.

increase in unsaturated as compared to saturated lipid vesicles [39]. Our present data show that the fluorescence spectra of F2N8 and F4N1 probes are also strongly dependent on the unsaturation level of the bilayer lipids (Fig. 7A,D). Thus, when vesicles made from unsaturated lipids (DOPC, EYPC) are compared with those made from saturated ones (DLPC, DMPC and DPPC) in their liquid crystalline phase, both probes show a significantly higher I_{N*}/I_{T*} ratio (Table 2). This suggests that, as expected, the bilayer polarity increases with the level of unsaturation. In the meantime, the degree of hydration deduced from the F_B/F_F ratio is considerably higher only for the case of unsaturated DOPC vesicles at 20 °C, as compared with saturated DLPC vesicles at 25 °C (Table 2), while the hydration parameter is very close when EYPC and DLPC vesicles are compared. Importantly, for unsaturated lipid bilayers the excitation spectrum maximum is shifted to the red by 4–5 nm with respect to that in saturated lipids bilayers (Table 1). According to what is observed in model organic solvents [35], this red shift cannot be a result of changes in the polarity, but may be attributed to an increase in the electronic polarizability of the probe surrounding [35]. Evidently, this electronic polarizability increase is connected with the presence in the unsaturated lipids of double bonds with highly polarizable π-electrons. Thus, the present analysis in addition to polarity and hydration can provide an estimation of the presence of unsaturated bonds in the bilayer.

3.3.4. Effects of changes in the dipole potential gradients

As probe F4N1 possesses a vertical orientation in the bilayer, its emission should be sensitive to vertically oriented electric fields in the bilayer. Indeed, as it was recently shown, probe F4N1 and its analog with a reversed orientation show a strong sensitivity to the bilayer dipole potential [44]. As a consequence, addition of 30% 6-ketocholestanol to EYPC vesicles, which increases the bilayer dipole potential [2], decreases strongly the relative intensity of the short-wavelength band of F4N1 probe (Fig. 7E). Presently, we attempt to study this response in further detail by our new analysis. The results show that addition of 30% 6-ketocholestanol induces a strong (2.7-fold) decrease in the I_{N*}/I_{T*} ratio measured for probe F4N1 (Table 2). This decrease can be assigned to the electrochromic effect of the dipole potential that destabilizes the N* state and favors the forward ESIPT reaction and therefore the T* emission [44,55]. This electrochromic destabilization of the normal excited state (N*) can also be directly observed from the blue shifts of the excitation spectrum and the N* emission band (Fig. 7B,E; Table 1).

As expected from its non-parallel orientation to the dipole potential vector (Fig. 5), the probe F2N8 shows a smaller decrease of the I_{N*}/I_{T*} ratio (1.9-fold) than F4N1 upon addition of 6-ketocholestanol (Fig. 7B,E; Table 2). This smaller electrochromic effect observed with F2N8 is in line with the smaller shifts of the corresponding excitation and emission bands (Table 1). In addition, both probes show

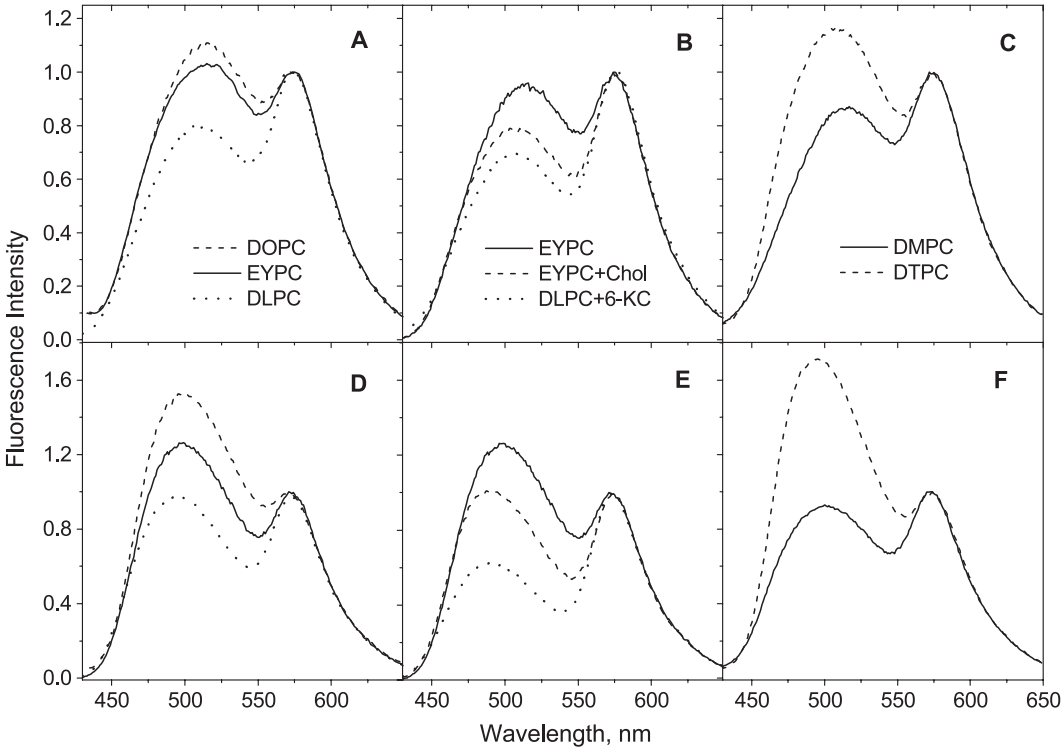

Fig. 7. Fluorescence response of the probes F2N8 (A–C) and F4N1 (D–F) to unsaturation degree and to cholesterol, 6-KC and ether lipids. (A and D) Fluorescence spectra of probes in LUV vesicles composed of EYPC (solid lines), DOPC (dashed lines) and DLPC (dots) at 25 °C; (B and E) EYPC with 30% of cholesterol (dashed line) and with 30% of 6-KC (dots); (C and F) DMPC (solid) and DTPC (dash) at 38 °C.

some decrease in the hydration parameter F_B/F_F (1.2- and 1.4-fold, for F2N8 and F4N1, respectively) with addition of 6-ketocholestanol, in line with the well-known dehydration effect of sterols [15,17].

In this respect, it was interesting to study the probe responses upon addition of cholesterol (Fig. 7B,E), which, though strongly modifying many membrane properties, increases the bilayer dipole potential only to a small extent [56]. Addition of 30% cholesterol to EYPC vesicles results in a 1.5-fold decrease in the I_{N*}/I_{T*} ratio for both probes. However, in both cases, no shift in the excitation maximum was observed. These results strongly suggest that the changes of the I_{N*}/I_{T*} ratio are not connected to the changes of dipole potential, but are predominantly due to the decrease in polarity of the bilayer. Thus, at 9.5 as well as at 13 Å from the bilayer center, the polarity decrease is of similar strong magnitude and can be assigned to the decrease in mobility of the ester groups of the bilayer as well as to the decreased amount and dielectric relaxation rate of water molecules. Additionally, dehydration of the bilayer upon addition of cholesterol is clearly seen from the decrease in the F_B/F_F ratio for both probes. However, the decrease of this ratio is significantly greater with probe F4N1 than with probe F2N8 (1.5-fold vs. 1.2-fold, respectively), showing that cholesterol dehydrates the bilayer more efficiently at deeper locations.

The substitution of ester lipids by ether analogs is another way to modify the dipole potential of lipid vesicles. In contrast to the addition of 6-KC, this substitution decreases the dipole potential [3]. Our data show that in DTPC vesicles, both in their gel and liquid crystalline phases, probes F4N1 and F2N8 show a strong increase of the I_{N*}/I_{T*} ratio with respect to DMPC vesicles (Fig. 7C,F; Table 2) as well as a strong red shift of the excitation spectrum (Table 1). Both effects are opposite to those occurring after addition of 6-KC, demonstrating that probes F2N8 and F4N1 respond to the dipole potential changes. In this case also, the spectroscopic response of probe F4N1, presenting a more vertical orientation in the bilayer as compared to F2N8, is significantly larger (Fig. 7C,F), with a 10 nm red shift of excitation spectrum vs. 7 nm, and a 2-fold I_{N*}/I_{T*} ratio increase vs. 1.8-fold (Tables 1 and 2). Finally, both probes show significantly decreased values of the hydration parameter F_B/F_F for DTPC as compared to DMPC vesicles in both their gel and liquid crystalline phases (Table 2).

4. Discussion

4.1. Probing methodology and its limitations

The present work is one of the first attempts to study simultaneously universal (dipole–dipole) and specific (H-bonding) interactions in lipid bilayers by a fluorescence method. For this purpose, we selected probes of 3-hydrox-

yflavone family that provide additional spectroscopic information on the intermolecular interactions [35] as compared to the commonly used solvatochromic dyes. From their fluorescence spectrum, it is possible to identify the presence and the relative amount of their H-bonded and H-bond-free forms. Recently, we showed that the H-bonded (to water) form of probe F locates much shallower in the bilayer than its H-bond-free form. More generally, we concluded that neutral dyes, which are not anchored in the lipid bilayer but capable of H-bonding interaction with water, undergo a bimodal distribution within the bilayer [39]. In this case, the concentration ratio of H-bonded to H-bond-free forms depends both on the bilayer hydration and on the probe location, as determined from the affinity of the probe for the various sites. Fixing the probe at particular depth and orientation would allow to estimate the bilayer hydration directly from the [H-bonded form]/[H-bond-free form] ratio. To address this point, we used the flavone dyes F2N8 and F4N1 bearing anchoring ammonium groups. Our results show that at least for the case of F2N8, this task was successfully realized, so that H-bonded form and H-bond-free form were fixed in nearly the same position (Fig. 5). To characterize the spectroscopic response of these probes we use two parameters. The first one is the intensity ratio of the N* and T* emission bands, I_{N*}/I_{T*}, which is an indicator of the site polarity of the non-H-bonded form of the flavone probe [35,39]. The second one is the ratio of integral intensities of the H-bonded to the non-H-bonded form of the probe, F_B/F_F, which describes the hydration. These two parameters can be obtained from the deconvolution of the probe fluorescence spectra into three emission bands: N*, H-N* and T*. The presence of these three bands was evidenced in the present work from the excitation wavelength dependence of the emission spectra, the emission anisotropy spectra and the effects of site-selective quenchers.

In spite of the anchoring group, the H-bonded forms of the probes (especially for F4N1) were found to be somewhat shallower located than the H-bond-free forms. This can be explained by the flickering of the probe around the anchoring ammonium group in the bilayer (Fig. 5). This may be a general trend for all solvatochromic probes and labels providing H-bonding interactions [39] and having enough freedom to relocate in the bilayer. The disparity in the location of the H-bonded and H-bond-free forms of the probes probably limits the resolution of our method to follow membrane hydration, which in the case of probes F2N8 and F4N1 is 3 Å (i.e. measured between 13 and 16 Å) and 8 Å (i.e. measured between 9.5 and 17 Å), respectively. It should be noted that the resolution of polarity measurement is limited by the size of the fluorophore, which is ca. 10 Å. Thus, both hydration and polarity measurements have similar resolutions, the only difference is that the polarity is followed at the depth of the H-bond-free forms, while hydration is followed between the locations of the H-bond-free and H-bonded forms.

4.2. Dielectric and hydration properties of lipid bilayer

The polarity of the bilayer measured with solvatochromic probes is an integrative parameter, taking into account both static and dynamic dielectric properties of the surroundings [1,11]. In lipid bilayers, the static dielectric properties are determined by the presence of sn_1 and sn_2 ester groups, double bonds of fatty acids and also of water molecules. Moreover, the polarization of these dipolar components is the background for the formation of the dipole potential [2], which can be considered as a vectorial component of the bilayer polarity. In the meantime, the dynamic dielectric properties are influenced by the mobility of the dipolar components (in other words, by rates of solvent relaxation [16,17,33]), i.e. by the fluidity of the corresponding region of the bilayer. Therefore, the polarity of the bilayer detected by our probes is a superposition of mainly three factors: fluidity, dipole potential, and hydration (or the presence of other polar components). Our data show that, in lipid bilayers of different compositions, the contribution of these three factors to polarity changes may be different.

Fluidity appears as a major contributor to polarity changes in the bilayer. Indeed, according to fluorescence anisotropy data obtained with DPH and TMA-DPH (1-[4-(trimethylammonio)phenyl]-6-phenyl-1,3,5-hexatriene probes, the increase in lipid unsaturation as well as the transition to the liquid crystalline phase significantly increase the fluidity of both the hydrophobic and the surface regions of the bilayer, while the addition of cholesterol produces the opposite effect [57,58]. According to our data with F2N8 and F4N1 probes, the bilayer polarity follows the same trends as the fluidity. Moreover, our experiments with saturated lipid bilayers at ‘‘equivalent temperature’’ further show that vesicles with a similar fluidity present a similar polarity (Table 2). In addition, the strong correlation between the solvation dynamics and the structure of the bilayer observed in our data is also in line with the data obtained with other solvatochromic probes, such as Prodan and Laurdan [14–17], showing that phase transition induces a strong increase in the solvent relaxation rates, while cholesterol produces the opposite effect.

The effects of dipole potential are observed only with strong dipole potential modifiers, such as 6-KC and ether lipids. The bilayer dipole potential, being parallel to the excited state dipole moment of the present probes, provides a negative contribution to the recorded polarity. In this respect, an increase of the dipole potential with addition of 6-KC induces a decrease in the polarity parameter I_{N*}/I_{T*}, while its decrease in the presence of ether lipids produces the opposite effect. Noticeably, the dipole potential effect can be distinguished from the other polarity effects by the shifts in the excitation spectra that accompany the strong changes in the I_{N*}/I_{T*} ratio, and by the stronger response of the vertically oriented F4N1 with respect to F2N8.

The presence of double bonds in lipid bilayers provides an additional contribution to the polarity due to an increase in the electronic polarizability of the hydrophobic region. This increase in electronic polarizability can be detected as a red shift in the excitation spectra of both probes, which is apparently similar to the effect of the decrease in the dipole potential (Table 2). Very similar spectroscopic effects reported with styryl electrochromic dyes di-8-ANEPPS and RH 421 were interpreted as a direct effect of lipid unsaturation on the dipole potential [59].

Since water molecules are highly polar, the bilayer polarity should also depend on its hydration [60,61]. A correlation between the polarity parameter I_{N*}/I_{T*} and the hydration parameter F_B/F_F is observed for phase transition and addition of cholesterol (Table 2), suggesting that, at least in these two cases, the changes in hydration contribute strongly to the changes in polarity. This is in line with the literature [60–62], showing that an increase in the hydration of the bilayer hydrophobic region may increase the polarity of this region. Furthermore, it was reported that an increase in the hydration is strongly connected to a decrease of the membrane lipid order (i.e. increase in fluidity) following phase transition, an increase in lipid unsaturation degree and a decrease of cholesterol content [20,58,63,64]. Thus, in these cases, polarity, hydration and lipid order appear as strongly related membrane parameters.

However, in some cases, the hydration profile appears rather independent from the polarity profile. For instance, an increase of temperature within the fluid phase for both saturated and unsaturated lipids vesicles strongly increases the bilayer hydration but does not significantly affect its polarity (Table 2). The same effect is observed when the bilayer curvature increases. Furthermore, in ether lipid vesicles, polarity and hydration are completely uncoupled as the strong increase of the polarity parameter I_{N*}/I_{T*} is accompanied by a strong decrease in the hydration parameter F_B/F_F. According to the literature, ether lipid vesicles are characterized by a high polarity [65], which has been assigned to their high hydration level. The present results strongly suggest that this high polarity may be connected in fact with the dielectric properties of the ether lipid vesicles (i.e. with the strongly decreased dipole potential).

Why can hydration and polarity of lipid bilayers in some cases be uncoupled? One reason could be that some polarity effectors (see above) give spectroscopic effects opposite to that of hydration. Another factor is that hydration, as determined by our dyes, is not a function of the total concentration of water in the bilayer but of the concentration of "free water" interacting with the probe. Evidently, by increasing either the temperature or the bilayer curvature, the "free water" concentration may significantly increase, resulting in an increased hydration. Obviously, this increase in hydration should be more pronounced at the interface of the bilayer than in its hydrophobic region. Since the H-bonded forms of the dyes locate shallower in the bilayer than the H-bond-free forms, a strong increase of the hydration at the interface may not be associated with a polarity increase in the deeper region of the bilayer. In line with this hypothesis, we observe for SUV and LUV a similar polarity of the hydrophobic region at 9–13 Å from the bilayer center. This is in line with data obtained with deeply located probes such as 12-AS (12-(9-anthroyloxy)-stearic acid) and DPH-phosphatidylcholine showing that the molecular order of the hydrophobic region is weakly dependent on the bilayer curvature [66,67]. In the meantime, the increased hydration reported with our dyes in SUV as compared to LUV corresponds to the shallower location, around 13–16 Å from the bilayer center. This is in full agreement with data obtained with shallow located probes such as TNS (2-*p*-toluidinyl-naphthalene-6-sulfonic acid), 2-AS (2-(9-anthroyloxy) stearic acid) and TMA-DPH showing that the interface of SUV is characterized by a faster solvent relaxation [66], a faster rotational motion and a higher hydration (and polarity) than the interface of LUV [67,68]. A similar interpretation can be provided for the temperature effects. Indeed, our data with saturated phospholipid vesicles at "equivalent temperatures" show that, for the same fluidity, the polarity of the hydrophobic region remains nearly the same, independently on the strong variations of the hydration at the interface (Fig. 6). In the case of unsaturated vesicles like EYPC vesicles, it is known that their fluidity is poorly sensitive to temperature variations [64]. Thus, the polarity of their hydrophobic region does not vary significantly with temperature, while the hydration of their interface may change dramatically (Table 2).

In conclusion, the present methodology applying two-band ratiometric 3-hydroxyflavone probes anchored at the membrane surface by charged groups allows a simultaneous analysis of bilayer polarity and hydration. This methodology provides interesting information on the relationship between these two parameters for lipid bilayers of different composition in various conditions. Our results confirm that the polarity of the bilayer at a depth of 9.5–13 Å from the bilayer center (corresponding to the locations of the H-bond-free forms of probes F4N1 and F2N8) could be strongly decreased by increasing the lipid order in the region of ester groups and acyl chains, i.e. on phase transition from fluid to gel phase, on decrease in lipid unsaturation and with addition of cholesterol. In these cases, the decrease in polarity is accompanied by a decrease in the bilayer hydration, especially for addition of cholesterol. In the other cases, the polarity and the hydration are completely uncoupled. For instance, in the case where fluidity is kept invariant at "equivalent temperatures" for saturated lipids, a higher temperature leads to a higher bilayer hydration but keeps the polarity unchanged. The same phenomenon is observed with the increase of the bilayer curvature. Furthermore, the data obtained after addition of 6-ketocholestanol and with ether lipids show that strong variations of dipole potential, a vectorial component of the bilayer polarity, may not correlate with the hydration.

Acknowledgements

This work was supported by grants from CNRS, Université Louis Pasteur, Strasbourg (France), TUBITAK (Turkey) and the French–Ukrainian *Programme d'action intégré* DNIPRO. Alexander Demchenko and Andrey Klymchenko acknowledge the fellowships from the Université Louis Pasteur and CNRS, respectively.

References

[1] G. Cevc, D. Marsh, Phospholipid Bilayers. Physical Principles and Models, Wiley, New York, 1987.
[2] J.C Franklin, D.S. Cafiso, Internal electrostatic potentials in bilayers: measuring and controlling dipole potentials in lipid vesicles, Biophys. J. 65 (1993) 289–299.
[3] K. Gawrisch, D. Ruston, J. Zimmerberg, V.A. Parsegian, R.P. Rand, N. Fuller, Membrane dipole potentials, hydration forces, and the ordering of water at membrane surfaces, Biophys. J. 61 (1992) 1213–1223.
[4] R.R. Gabdoulline, C. Zheng, G. Vanderkooi, Molecular origin of the internal dipole potential in lipid bilayers: role of the electrostatic potential of water, Chem. Phys. Lipids 84 (1996) 139–146.
[5] J. Cladera, P. O'Shea, Intramembrane molecular dipoles affect the membrane insertion and folding of a model amphiphilic peptide, Biophys. J. 74 (1998) 2434–2442.
[6] L. Voglino, T.J. McIntosh, S.A. Simon, Modulation of the binding of signal peptides to lipid bilayers by dipoles near the hydrocarbon–water interface, Biochemistry 37 (1998) 12241–12252.
[7] D. Marsh, Polarity and permeation profiles in lipid membranes, Proc. Natl. Acad. Sci. U. S. A. 98 (2001) 7777–7782.
[8] R. Bartucci, R. Guzzi, D. Marsh, L. Sportelli, Intramembrane polarity by electron spin echo spectroscopy of labeled lipids, Biophys. J. 84 (2003) 1025–1030.
[9] F. Volke, S. Eisenblätter, G. Klose, Hydration force parameters of phosphatidylcholine lipid bilayer as determined from 2H-NMR studies of deuterated water, Biophys. J. 67 (1994) 1882–1887.
[10] J.F. Nagle, Y. Liu, S. Tristram-Nagle, R.M. Epand, R.E. Stark, Reanalysis of magic angle spinning nuclear magnetic resonance determination of interlamellar waters in lipid bilayer dispersions, Biophys. J. 77 (1999) 2062–2065.
[11] W. Hübner, A. Blume, Interactions at the lipid–water interface, Chem. Phys. Lipids 96 (1998) 99–123.
[12] P.T.T. Wong, H.H. Mantsch, High-pressure infrared spectroscopic evidence of water binding sites in 1,2-diacyl phospholipids, Chem. Phys. Lipids 46 (1988) 213–224.
[13] B. Valeur, Molecular Fluorescence, Wiley, Weinheim, 2002.
[14] E.K. Krasnowska, E. Gratton, T. Parasassi, Prodan as a membrane surface fluorescence probe: partitioning between water and phospholipid phases, Biophys. J. 74 (1998) 1984–1993.
[15] J.B. Massey, Effect of cholesteryl hemisuccinate on the interfacial properties of phosphatidylcholine bilayers, Biochim. Biophys. Acta 1415 (1998) 193–204.
[16] T. Parasassi, G. De Stasio, A. d'Ubaldo, E. Gratton, Phase fluctuation in phospholipid membranes revealed by Laurdan fluorescence, Biophys. J. 57 (1990) 1179–1186.
[17] T. Parasassi, M. Di Stefano, M. Loiero, G. Ravagnan, E. Gratton, Cholesterol modifies water concentration and dynamics in phospholipid bilayers: a fluorescence study using Laurdan probe, Biophys. J. 66 (1994) 763–768.
[18] J.M.I. Alakoskela, P.K.J. Kinnunen, Probing phospholipid main phase transition by fluorescence spectroscopy and a surface redox reaction, J. Phys. Chem., B 105 (2001) 11294–11301.
[19] A. Chattopadhyay, S. Mukherjee, Red edge excitation shift of a deeply embedded membrane probe: implications in water penetration in the bilayer, J. Phys. Chem., B 103 (1999) 8180–8185.
[20] C. Ho, S.J. Slater, C.D. Stubbs, Hydration and order in lipid bilayers, Biochemistry 34 (1995) 6188–6195.
[21] D.L. Bernik, D. Zubiri, E. Tymczyszyn, E.A. Disalvo, Polarity and packing at the carbonyl and phosphate regions of lipid bilayers, Langmuir 17 (2001) 6438–6442.
[22] E. Asuncion-Punzalan, K. Kachel, E. London, Groups with polar characteristics can locate at both shallow and deep locations in membranes: the behavior of dansyl and related probes, Biochemistry 37 (1998) 4603–4611.
[23] F.S. Abrams, A. Chattopadhyay, E. London, Determination of the location of fluorescent probes attached to fatty acids using parallax analysis of fluorescence quenching: effect of carboxyl ionization state and environment on depth, Biochemistry 31 (1992) 5322–5327.
[24] A. Chattopadhyay, S. Mukherjee, Depth-dependent solvent relaxation in membranes: wavelength-selective fluorescence as a membrane dipstick, Langmuir 15 (1999) 2142–2148.
[25] N.G. Bakhshiev, Spectroscopy of Intermolecular Interactions, Nauka, Leningrad, 1972.
[26] E.L. Lippert, Laser-spectroscopic studies of reorientation and other relaxation processes in solution, in: J.B. Birks (Ed.), Organic Molecular Photophysics, vol. 2, Wiley, New York, 1975, pp. 1–31.
[27] C. Reichardt, Solvatochromic dyes as solvent polarity indicators, Chem. Rev. 94 (1994) 2319–2358.
[28] J. Catalan, P. Perez, J. Laynez, F.G. Blanco, Analysis of the solvent effect on the photophysics properties of 6-propionyl-2-(dimethylamino)naphthalene (PRODAN), J. Fluoresc. 1 (1991) 215–223.
[29] F.M. Cerezo, S.C. Rocafort, P.S. Sierra, F. Garcia-Blanco, C.D. Oliva, J.C. Sierra, Photophysical study of the probes acrylodan (1-[6-(dimethylamino)naphthalen-2-yl]prop-2-en-1-one), ANS (8-anilinonaphthalene-1-sulfonate) and Prodan (1-[6-(dimethylamino)naphthalen-2-yl]propan-1-one) in aqueous mixtures of various alcohols, Helv. Chim. Acta 84 (2001) 3306–3312.
[30] B.E. Cohen, T.B. McAnaney, E.S. Park, Y.N. Jan, S.G. Boxer, L.Y. Jan, Probing protein electrostatics with a synthetic fluorescent amino acid, Science 296 (2002) 1700–1703.
[31] M.J. Kamlet, R.W. Taft, P.W. Carr, M.H. Abraham, Linear solvation energy relationships, J. Chem. Soc., Faraday Trans. I 78 (1982) 1689–1704.
[32] M.H. Abraham, H.S. Chadha, G.S. Whiting, R.C. Mitchell, Hydrogen bonding. Part 32. An analysis of water–octanol and water–alkane partitioning, and the DlogP parameter of Seiler, J. Pharm. Sci. 83 (1994) 1085–1100.
[33] J. Gardecki, M.L. Horng, A. Papazyan, M. Maroncelli, Ultrafast measurements of the dynamics of solvation in polar and non-dipolar solvents, J. Mol. Liq. 65–66 (1995) 49–57.
[34] P.K. Sengupta, M. Kasha, Excited state proton-transfer spectroscopy of 3-hydroxyflavone and quercetin, Chem. Phys. Lett. 68 (1979) 382–385.
[35] A.S. Klymchenko, A.P. Demchenko, Multiparametric probing of intermolecular interactions with fluorescent dye exhibiting excited state intramolecular proton transfer, Phys. Chem. Chem. Phys. 5 (2003) 461–468.
[36] A.S. Klymchenko, V.G. Pivovarenko, A.P. Demchenko, Elimination of hydrogen bonding effect on solvatochromism of 3-hydroxyflavones, J. Phys. Chem., A 107 (2003) 4211–4216.
[37] O.P. Bondar, V.G. Pivovarenko, E.S. Rowe, Flavonols: new fluorescent membrane probes for studying the interdigitation of lipid bilayers, Biochim. Biophys. Acta 1369 (1998) 119–130.
[38] G. Duportail, A. Klymchenko, Y. Mély, A. Demchenko, Neutral fluorescence probe with strong ratiometric response to surface charge of phospholipid membranes, FEBS Lett. 508 (2001) 196–200.
[39] A.S. Klymchenko, G. Duportail, A.P. Demchenko, Y. Mély, Bimodal distribution and fluorescence response of environment-sensitive probes in lipid bilayers, Biophys. J. 86 (2004) 2929–2941.
[40] J.R. Lakowicz, D.R. Bevan, B.P. Maliwal, H. Cherek, A. Balter,

Synthesis and characterization of a fluorescence probe of the phase transition and dynamic properties of membranes, Biochemistry 22 (1983) 5714–5722.
[41] R. Kraayenhof, G.J. Sterk, H.W. Wong Fong Sang, Probing biomembrane interface potential and pH profiles with a new type of float-like fluorophores positioned at varying distance from the membrane surface, Biochemistry 32 (1993) 10057–10066.
[42] L.M. Loew, Design and characterization of electrochromic membrane probes, J. Biochem. Biophys. Methods 6 (1982) 243–260.
[43] A.S. Klymchenko, G. Duportail, T. Oztürk, V.G. Pivovarenko, Y. Mély, A.P. Demchenko, Novel two-band ratiometric fluorescence probes with different location and orientation in phospholipid membranes, Chem. Biol. 9 (2002) 1199–1208.
[44] A.S. Klymchenko, G. Duportail, Y. Mély, A.P. Demchenko, Ultrasensitive two-color fluorescence probes for dipole potential in phospholipid membranes, Proc. Natl. Acad. Sci. U. S. A. 100 (2003) 11219–11224.
[45] M.J. Hope, M.B. Bally, G. Webb, P.R. Cullis, Production of large unilamellar vesicles by a rapid extrusion procedure. Characterization of size distribution, trapped volume and ability to maintain a membrane potential, Biochim. Biophys. Acta 812 (1985) 55–65.
[46] A. Chattopadhyay, E. London, Parallax method for direct measurement of membrane penetration depth utilizing fluorescence quenching by spin-labeled phospholipids, Biochemistry 26 (1987) 39–45.
[47] F.S. Abrams, E. London, Extension of the parallax analysis of membrane penetration depth to the polar region of model membranes: use of fluorescence quenching by a spin-label attached to the phospholipid polar headgroup, Biochemistry 32 (1993) 10826–10831.
[48] A.O. Doroshenko, L.B. Sychevskaya, A.V. Grygorovych, V.G. Pivovarenko, Fluorescence probing of cell membranes with azacrown substituted ketocyanine dyes, J. Fluoresc. 12 (2002) 455–464.
[49] D.B. Siano, D.E. Metzler, Band shapes of the electronic spectra of complex molecules, J. Chem. Phys. 51 (1969) 1856–1861.
[50] C.M. Metzler, A.E. Cahill, S. Petty, D.E. Metzler, L. Lang, The widespread applicability of log-normal curves for the description of absorption spectra, Appl. Spectrosc. 39 (1985) 333–339.
[51] C.M. Viswanath, D.E. Metzler, Equilibria and absorption spectra of tryptophanase, J. Biol. Chem. 266 (1991) 9374–9381.
[52] E.A. Burstein, S.M. Abornev, Y.K. Reshetnyak, Decomposition of protein tryptophan fluorescence spectra into log-normal components: I. Decomposition algorithms, Biophys. J. 81 (2001) 1699–1709.
[53] A.P. Demchenko, The red-edge effects: 30 years of exploration, Luminescence 17 (2002) 19–42.
[54] M.C. Wiener, S.H. White, Structure of a fluid dioleoylphosphatidylcholine bilayer determined by joint refinement of X-ray and neutron diffraction: III. Complete structure, Biophys. J. 61 (1992) 434–447.
[55] A.S. Klymchenko, A.P. Demchenko, Electrochromic modulation of excited-state intramolecular proton transfer: the new principle in design of fluorescence sensors, J. Am. Chem. Soc. 124 (2002) 12372–12379.
[56] E. Gross, R.S. Bedlack Jr., L.M. Loew, Dual-wavelength ratiometric fluorescence measurement of the membrane dipole potential, Biophys. J. 67 (1994) 208–216.
[57] W.J. Van Blitterswijk, B.W. Van der Meer, H. Hilkmann, Quantitative contributions of cholesterol and the individual classes of phospholipids and their degree of fatty acyl (un)saturation to membrane fluidity measured by fluorescence polarization, Biochemistry 26 (1987) 1746–1756.
[58] M. Straume, B.J. Litman, Influence of cholesterol on equilibrium and dynamic bilayer structure of unsaturated acyl chain phosphatidylcholine vesicles as determined from higher order analysis of fluorescence anisotropy decay, Biochemistry 26 (1987) 5121–5126.
[59] R.J. Clarke, Effect of lipid structure on the dipole potential of phosphatidylcholine bilayers, Biochim. Biophys. Acta 1327 (1997) 269–278.
[60] D. Kurad, G. Jeschke, D. Marsh, Lipid membrane polarity profiles by high-field EPR, Biophys. J. 85 (2003) 1025–1033.
[61] R. Bartucci, R. Guzzi, D. Marsh, L. Sportelli, Intramembrane polarity by electron spin echo spectroscopy of labeled lipids, Biophys. J. 84 (2003) 1025–1030.
[62] E. Pérochon, A. Lopez, J.F. Tocanne, Polarity of lipid bilayers. A fluorescence investigation, Biochemistry 31 (1992) 7672–7682.
[63] T.H. Haines, Water transport across biological membranes, FEBS Lett. 346 (1994) 115–122.
[64] H. Binder, K. Gawrisch, Effect of unsaturated lipid chains on dimensions, molecular order and hydration of membranes, J. Phys. Chem., B 105 (2001) 12378–12390.
[65] R. Hutterer, M. Hof, Dynamics in diether lipid bilayers and interdigitated bilayer structures studied by time-resolved emission spectra, decay time and anisotropy profiles, J. Fluoresc. 11 (2001) 227–236.
[66] M. Hof, R. Hutterer, N. Pérez, H. Ruf, F.W. Schneider, Influence of vesicle curvature on fluorescence relaxation kinetics of fluorophores, Biophys. Chem. 52 (1994) 165–172.
[67] G.W. Hunter, T.C. Squier, Phospholipid acyl chain rotational dynamics are independent of headgroup structure in unilamellar vesicles containing binary mixtures of dioleoyl-phosphatidylcholine and dioleoyl-phosphatidylethanolamine, Biochim. Biophys. Acta 1415 (1998) 63–76.
[68] W.A. Talbot, L.X. Zheng, B.R. Lentz, Acyl chain unsaturation and vesicle curvature alter outer leaflet packing and promote poly(ethylene glycol)-mediated membrane fusion, Biochemistry 36 (1997) 5827–5836.